

Search for a light CP-odd Higgs boson in the radiative decays of J/ψ

M. Ablikim¹, M. N. Achasov^{9,f}, X. C. Ai¹, O. Albayrak⁵, M. Albrecht⁴, D. J. Ambrose⁴⁴, A. Amoroso^{49A,49C}, F. F. An¹, Q. An^{46,a}, J. Z. Bai¹, R. Baldini Ferroli^{20A}, Y. Ban³¹, D. W. Bennett¹⁹, J. V. Bennett⁵, M. Bertani^{20A}, D. Bettoni^{21A}, J. M. Bian⁴³, F. Bianchi^{49A,49C}, E. Boger^{23,d}, I. Boyko²³, R. A. Briere⁵, H. Cai⁵¹, X. Cai^{1,a}, O. Cakir^{40A,b}, A. Calcaterra^{20A}, G. F. Cao¹, S. A. Cetin^{40B}, J. F. Chang^{1,a}, G. Chelkov^{23,d,e}, G. Chen¹, H. S. Chen¹, H. Y. Chen², J. C. Chen¹, M. L. Chen^{1,a}, S. J. Chen²⁹, X. Chen^{1,a}, X. R. Chen²⁶, Y. B. Chen^{1,a}, H. P. Cheng¹⁷, X. K. Chu³¹, G. Cibinetto^{21A}, H. L. Dai^{1,a}, J. P. Dai³⁴, A. Dbeysy¹⁴, D. Dedovich²³, Z. Y. Deng¹, A. Denig²², I. Denysenko²³, M. Destefanis^{49A,49C}, F. De Mori^{49A,49C}, Y. Ding²⁷, C. Dong³⁰, J. Dong^{1,a}, L. Y. Dong¹, M. Y. Dong^{1,a}, Z. L. Dou²⁹, S. X. Du⁵³, P. F. Duan¹, J. Z. Fan³⁹, J. Fang^{1,a}, S. S. Fang¹, X. Fang^{46,a}, Y. Fang¹, L. Fava^{49B,49C}, F. Feldbauer²², G. Felici^{20A}, C. Q. Feng^{46,a}, E. Fioravanti^{21A}, M. Fritsch^{14,22}, C. D. Fu¹, Q. Gao¹, X. L. Gao^{46,a}, X. Y. Gao², Y. Gao³⁹, Z. Gao^{46,a}, I. Garzia^{21A}, K. Goetzen¹⁰, W. X. Gong^{1,a}, W. Gradl²², M. Greco^{49A,49C}, M. H. Gu^{1,a}, Y. T. Gu¹², Y. H. Guan¹, A. Q. Guo¹, L. B. Guo²⁸, Y. Guo¹, Y. P. Guo²², Z. Haddadi²⁵, A. Hafner²², S. Han⁵¹, F. A. Harris⁴², K. L. He¹, T. Held⁴, Y. K. Heng^{1,a}, Z. L. Hou¹, C. Hu²⁸, H. M. Hu¹, J. F. Hu^{49A,49C}, T. Hu^{1,a}, Y. Hu¹, G. M. Huang⁶, G. S. Huang^{46,a}, J. S. Huang¹⁵, X. T. Huang³³, Y. Huang²⁹, T. Hussain⁴⁸, Q. Ji¹, Q. P. Ji³⁰, X. B. Ji¹, X. L. Ji^{1,a}, L. W. Jiang⁵¹, X. S. Jiang^{1,a}, X. Y. Jiang³⁰, J. B. Jiao³³, Z. Jiao¹⁷, D. P. Jin^{1,a}, S. Jin¹, T. Johansson⁵⁰, A. Julin⁴³, N. Kalantar-Nayestanaki²⁵, X. L. Kang¹, X. S. Kang³⁰, M. Kavatsyuk²⁵, B. C. Ke⁵, P. Kiese²², R. Kliemt¹⁴, B. Kloss²², O. B. Kolcu^{40B,i}, B. Kopf⁴, M. Kornicer⁴², W. Kühn²⁴, A. Kupsc⁵⁰, J. S. Lange²⁴, M. Lara¹⁹, P. Larin¹⁴, C. Leng^{49C}, C. Li⁵⁰, Cheng Li^{46,a}, D. M. Li⁵³, F. Li^{1,a}, F. Y. Li³¹, G. Li¹, H. B. Li¹, J. C. Li¹, Jin Li³², K. Li¹³, K. Li³³, Lei Li³, P. R. Li⁴¹, T. Li³³, W. D. Li¹, W. G. Li¹, X. L. Li³³, X. M. Li¹², X. N. Li^{1,a}, X. Q. Li³⁰, Z. B. Li³⁸, H. Liang^{46,a}, Y. F. Liang³⁶, Y. T. Liang²⁴, G. R. Liao¹¹, D. X. Lin¹⁴, B. J. Liu¹, C. X. Liu¹, D. Liu^{46,a}, F. H. Liu³⁵, Fang Liu¹, Feng Liu⁶, H. B. Liu¹², H. H. Liu¹, H. H. Liu¹⁶, H. M. Liu¹, J. Liu¹, J. B. Liu^{46,a}, J. P. Liu⁵¹, J. Y. Liu¹, K. Liu³⁹, K. Y. Liu²⁷, L. D. Liu³¹, P. L. Liu^{1,a}, Q. Liu⁴¹, S. B. Liu^{46,a}, X. Liu²⁶, Y. B. Liu³⁰, Z. A. Liu^{1,a}, Zhiqing Liu²², H. Loehner²⁵, X. C. Lou^{1,a,h}, H. J. Lu¹⁷, J. G. Lu^{1,a}, Y. Lu¹, Y. P. Lu^{1,a}, C. L. Luo²⁸, M. X. Luo⁵², T. Luo⁴², X. L. Luo^{1,a}, X. R. Lyu⁴¹, F. C. Ma²⁷, H. L. Ma¹, L. L. Ma³³, Q. M. Ma¹, T. Ma¹, X. N. Ma³⁰, X. Y. Ma^{1,a}, F. E. Maas¹⁴, M. Maggiora^{49A,49C}, Y. J. Mao³¹, Z. P. Mao¹, S. Marcello^{49A,49C}, J. G. Messchendorp²⁵, J. Min^{1,a}, R. E. Mitchell¹⁹, X. H. Mo^{1,a}, Y. J. Mo⁶, C. Morales Morales¹⁴, N. Yu. Muchnoi^{9,f}, H. Muramatsu⁴³, Y. Nefedov²³, F. Nerling¹⁴, I. B. Nikolaev^{9,f}, Z. Ning^{1,a}, S. Nisar⁸, S. L. Niu^{1,a}, X. Y. Niu¹, S. L. Olsen³², Q. Ouyang^{1,a}, S. Pacetti^{20B}, Y. Pan^{46,a}, P. Patteri^{20A}, M. Pelizaeus⁴, H. P. Peng^{46,a}, K. Peters¹⁰, J. Pettersson⁵⁰, J. L. Ping²⁸, R. G. Ping¹, R. Poling⁴³, V. Prasad¹, M. Qi²⁹, S. Qian^{1,a}, C. F. Qiao⁴¹, L. Q. Qin³³, N. Qin⁵¹, X. S. Qin¹, Z. H. Qin^{1,a}, J. F. Qiu¹, K. H. Rashid⁴⁸, C. F. Redmer²², M. Ripka²², G. Rong¹, Ch. Rosner¹⁴, X. D. Ruan¹², V. Santoro^{21A}, A. Sarantsev^{23,g}, M. Savrié^{21B}, K. Schoenning⁵⁰, S. Schumann²², W. Shan³¹, M. Shao^{46,a}, C. P. Shen², P. X. Shen³⁰, X. Y. Shen¹, H. Y. Sheng¹, W. M. Song¹, X. Y. Song¹, S. Sosio^{49A,49C}, S. Spataro^{49A,49C}, G. X. Sun¹, J. F. Sun¹⁵, S. S. Sun¹, Y. J. Sun^{46,a}, Y. Z. Sun¹, Z. J. Sun^{1,a}, Z. T. Sun¹⁹, C. J. Tang³⁶, X. Tang¹, I. Tapan^{40C}, E. H. Thorndike⁴⁴, M. Tiemens²⁵, M. Ullrich²⁴, I. Uman^{40B}, G. S. Varner⁴², B. Wang³⁰, B. L. Wang⁴¹, D. Wang³¹, D. Y. Wang³¹, K. Wang^{1,a}, L. L. Wang¹, L. S. Wang¹, M. Wang³³, P. Wang¹, P. L. Wang¹, S. G. Wang³¹, W. Wang^{1,a}, W. P. Wang^{46,a}, X. F. Wang³⁹, Y. D. Wang¹⁴, Y. F. Wang^{1,a}, Y. Q. Wang²², Z. Wang^{1,a}, Z. G. Wang^{1,a}, Z. H. Wang^{46,a}, Z. Y. Wang¹, T. Weber²², D. H. Wei¹, J. B. Wei³¹, P. Weidenkaff²², S. P. Wen¹, U. Wiedner⁴, M. Wolke⁵⁰, L. H. Wu¹, Z. Wu^{1,a}, L. Xia^{46,a}, L. G. Xia³⁹, Y. Xia¹⁸, D. Xiao¹, H. Xiao⁴⁷, Z. J. Xiao²⁸, Y. G. Xie^{1,a}, Q. L. Xiu^{1,a}, G. F. Xu¹, L. Xu¹, Q. J. Xu¹³, X. P. Xu³⁷, L. Yan^{49A,49C}, W. B. Yan^{46,a}, W. C. Yan^{46,a}, Y. H. Yan¹⁸, H. J. Yang³⁴, H. X. Yang¹, L. Yang⁵¹, Y. Yang⁶, Y. Y. Yang¹¹, M. Ye^{1,a}, M. H. Ye⁷, J. H. Yin¹, B. X. Yu^{1,a}, C. X. Yu³⁰, J. S. Yu²⁶, C. Z. Yuan¹, W. L. Yuan²⁹, Y. Yuan¹, A. Yuncu^{40B,c}, A. A. Zafar⁴⁸, A. Zallo^{20A}, Y. Zeng¹⁸, Z. Zeng^{46,a}, B. X. Zhang¹, B. Y. Zhang^{1,a}, C. Zhang²⁹, C. C. Zhang¹, D. H. Zhang¹, H. H. Zhang³⁸, H. Y. Zhang^{1,a}, J. J. Zhang¹, J. L. Zhang¹, J. Q. Zhang¹, J. W. Zhang^{1,a}, J. Y. Zhang¹, J. Z. Zhang¹, K. Zhang¹, L. Zhang¹, X. Y. Zhang³³, Y. Zhang¹, Y. H. Zhang^{1,a}, Y. N. Zhang⁴¹, Y. T. Zhang^{46,a}, Yu Zhang⁴¹, Z. H. Zhang⁶, Z. P. Zhang⁴⁶, Z. Y. Zhang⁵¹, G. Zhao¹, J. W. Zhao^{1,a}, J. Y. Zhao¹, J. Z. Zhao^{1,a}, Lei Zhao^{46,a}, Ling Zhao¹, M. G. Zhao³⁰, Q. Zhao¹, Q. W. Zhao¹, S. J. Zhao⁵³, T. C. Zhao¹, Y. B. Zhao^{1,a}, Z. G. Zhao^{46,a}, A. Zhemchugov^{23,d}, B. Zheng⁴⁷, J. P. Zheng^{1,a}, W. J. Zheng³³, Y. H. Zheng⁴¹, B. Zhong²⁸, L. Zhou^{1,a}, X. Zhou⁵¹, X. K. Zhou^{46,a}, X. R. Zhou^{46,a}, X. Y. Zhou¹, K. Zhu¹, K. J. Zhu^{1,a}, S. Zhu¹, S. H. Zhu⁴⁵, X. L. Zhu³⁹, Y. C. Zhu^{46,a}, Y. S. Zhu¹, Z. A. Zhu¹, J. Zhuang^{1,a}, L. Zotti^{49A,49C}, B. S. Zou¹, J. H. Zou¹

(BESIII Collaboration)

¹ Institute of High Energy Physics, Beijing 100049, People's Republic of China

² Beihang University, Beijing 100191, People's Republic of China

³ Beijing Institute of Petrochemical Technology, Beijing 102617, People's Republic of China

⁴ Bochum Ruhr-University, D-44780 Bochum, Germany

⁵ Carnegie Mellon University, Pittsburgh, Pennsylvania 15213, USA

⁶ Central China Normal University, Wuhan 430079, People's Republic of China

⁷ China Center of Advanced Science and Technology, Beijing 100190, People's Republic of China

⁸ COMSATS Institute of Information Technology, Lahore, Defence Road, Off Raiwind Road, 54000 Lahore, Pakistan

⁹ G.I. Budker Institute of Nuclear Physics SB RAS (BINP), Novosibirsk 630090, Russia

¹⁰ GSI Helmholtzcentre for Heavy Ion Research GmbH, D-64291 Darmstadt, Germany

¹¹ Guangxi Normal University, Guilin 541004, People's Republic of China

¹² GuangXi University, Nanning 530004, People's Republic of China

¹³ Hangzhou Normal University, Hangzhou 310036, People's Republic of China

- ¹⁴ *Helmholtz Institute Mainz, Johann-Joachim-Becher-Weg 45, D-55099 Mainz, Germany*
- ¹⁵ *Henan Normal University, Xinxiang 453007, People's Republic of China*
- ¹⁶ *Henan University of Science and Technology, Luoyang 471003, People's Republic of China*
- ¹⁷ *Huangshan College, Huangshan 245000, People's Republic of China*
- ¹⁸ *Hunan University, Changsha 410082, People's Republic of China*
- ¹⁹ *Indiana University, Bloomington, Indiana 47405, USA*
- ²⁰ (A)*INFN Laboratori Nazionali di Frascati, I-00044, Frascati, Italy; (B)INFN and University of Perugia, I-06100, Perugia, Italy*
- ²¹ (A)*INFN Sezione di Ferrara, I-44122, Ferrara, Italy; (B)University of Ferrara, I-44122, Ferrara, Italy*
- ²² *Johannes Gutenberg University of Mainz, Johann-Joachim-Becher-Weg 45, D-55099 Mainz, Germany*
- ²³ *Joint Institute for Nuclear Research, 141980 Dubna, Moscow region, Russia*
- ²⁴ *Justus Liebig University Giessen, II. Physikalisches Institut, Heinrich-Buff-Ring 16, D-35392 Giessen, Germany*
- ²⁵ *KVI-CART, University of Groningen, NL-9747 AA Groningen, The Netherlands*
- ²⁶ *Lanzhou University, Lanzhou 730000, People's Republic of China*
- ²⁷ *Liaoning University, Shenyang 110036, People's Republic of China*
- ²⁸ *Nanjing Normal University, Nanjing 210023, People's Republic of China*
- ²⁹ *Nanjing University, Nanjing 210093, People's Republic of China*
- ³⁰ *Nankai University, Tianjin 300071, People's Republic of China*
- ³¹ *Peking University, Beijing 100871, People's Republic of China*
- ³² *Seoul National University, Seoul, 151-747 Korea*
- ³³ *Shandong University, Jinan 250100, People's Republic of China*
- ³⁴ *Shanghai Jiao Tong University, Shanghai 200240, People's Republic of China*
- ³⁵ *Shanxi University, Taiyuan 030006, People's Republic of China*
- ³⁶ *Sichuan University, Chengdu 610064, People's Republic of China*
- ³⁷ *Soochow University, Suzhou 215006, People's Republic of China*
- ³⁸ *Sun Yat-Sen University, Guangzhou 510275, People's Republic of China*
- ³⁹ *Tsinghua University, Beijing 100084, People's Republic of China*
- ⁴⁰ (A)*Istanbul Aydin University, 34295 Sefakoy, Istanbul, Turkey; (B)Istanbul Bilgi University, 34060 Eyup, Istanbul, Turkey; (C)Uludag University, 16059 Bursa, Turkey*
- ⁴¹ *University of Chinese Academy of Sciences, Beijing 100049, People's Republic of China*
- ⁴² *University of Hawaii, Honolulu, Hawaii 96822, USA*
- ⁴³ *University of Minnesota, Minneapolis, Minnesota 55455, USA*
- ⁴⁴ *University of Rochester, Rochester, New York 14627, USA*
- ⁴⁵ *University of Science and Technology Liaoning, Anshan 114051, People's Republic of China*
- ⁴⁶ *University of Science and Technology of China, Hefei 230026, People's Republic of China*
- ⁴⁷ *University of South China, Hengyang 421001, People's Republic of China*
- ⁴⁸ *University of the Punjab, Lahore-54590, Pakistan*
- ⁴⁹ (A)*University of Turin, I-10125, Turin, Italy; (B)University of Eastern Piedmont, I-15121, Alessandria, Italy; (C)INFN, I-10125, Turin, Italy*
- ⁵⁰ *Uppsala University, Box 516, SE-75120 Uppsala, Sweden*
- ⁵¹ *Wuhan University, Wuhan 430072, People's Republic of China*
- ⁵² *Zhejiang University, Hangzhou 310027, People's Republic of China*
- ⁵³ *Zhengzhou University, Zhengzhou 450001, People's Republic of China*
- ^a *Also at State Key Laboratory of Particle Detection and Electronics, Beijing 100049, Hefei 230026, People's Republic of China*
- ^b *Also at Ankara University, 06100 Tandogan, Ankara, Turkey*
- ^c *Also at Bogazici University, 34342 Istanbul, Turkey*
- ^d *Also at the Moscow Institute of Physics and Technology, Moscow 141700, Russia*
- ^e *Also at the Functional Electronics Laboratory, Tomsk State University, Tomsk, 634050, Russia*
- ^f *Also at the Novosibirsk State University, Novosibirsk, 630090, Russia*
- ^g *Also at the NRC "Kurchatov Institute", PNPI, 188300, Gatchina, Russia*
- ^h *Also at University of Texas at Dallas, Richardson, Texas 75083, USA*
- ⁱ *Also at Istanbul Arel University, 34295 Istanbul, Turkey*

We search for a light Higgs boson A^0 in the fully reconstructed decay chain of $J/\psi \rightarrow \gamma A^0$, $A^0 \rightarrow \mu^+ \mu^-$ using $(225.0 \pm 2.8) \times 10^6$ J/ψ events collected by the BESIII experiment. The A^0 is a hypothetical CP-odd light Higgs boson predicted by many extensions of the Standard Model including two spin-0 doublets plus an extra singlet. We find no evidence for A^0 production and set 90% confidence-level upper limits on the product branching fraction $\mathcal{B}(J/\psi \rightarrow \gamma A^0) \times \mathcal{B}(A^0 \rightarrow \mu^+ \mu^-)$ in the range of $(2.8 - 495.3) \times 10^{-8}$ for $0.212 \leq m_{A^0} \leq 3.0$ GeV/ c^2 . The new limits are 5 times below our previous results, and the nature of the A^0 is constrained to be mostly singlet.

The radiative decays of the J/ψ have long been identified as a way to search for new particles such as a light scalar, a pseudo-scalar Higgs boson [1], or a light spin-1 gauge boson [2]. In particular a light CP-odd pseudo-scalar may be present in various models of physics beyond the Standard Model, such as the Next-to-Minimal Supersymmetric Standard Model (NMSSM) [3]. The NMSSM appends an additional singlet chiral superfield to the Minimal Supersymmetric Standard Model (MSSM) [4], in order to solve or alleviate the so-called ‘‘little hierarchy problem’’ [5]. It has a rich Higgs sector containing three CP-even, two CP-odd and two charged Higgs bosons. The mass of the lightest CP-odd Higgs boson, A^0 , may be less than twice the mass of the charmed quark.

The branching fraction of $V \rightarrow \gamma A^0$ ($V = \Upsilon, J/\psi$) is related to the Yukawa coupling of A^0 to the down or up type of quark (g_q^2) through [1, 6, 7],

$$\frac{\mathcal{B}(V \rightarrow \gamma A^0)}{\mathcal{B}(V \rightarrow l^+ l^-)} = \frac{G_F m_q^2 g_q^2 C_{QCD}}{\sqrt{2} \pi \alpha} \left(1 - \frac{m_{A^0}^2}{m_V^2} \right) \quad (1)$$

where $l \equiv e$ or μ , α is the fine structure constant, m_q the quark mass and C_{QCD} the combined m_{A^0} dependent QCD and relativistic corrections to $\mathcal{B}(V \rightarrow \gamma A^0)$ [7] and the leptonic width of $\mathcal{B}(V \rightarrow l^+ l^-)$ [8]. The correction of first order in the strong coupling constant (α_S) is as large as 30% [7] but comparable to the theoretical uncertainties [9]. In the NMSSM, $g_c = \cos \theta_A / \tan \beta$ for the c -quark and $g_b = \cos \theta_A \tan \beta$ for the b -quark, where $\tan \beta$ is the ratio of the expectation values of the up and down types of the Higgs doublets and $\cos \theta_A$ the fraction of the non-singlet component in the A^0 [10, 11]; $\cos \theta_A$ takes into account the doublet-singlet mixing and would be small for a mostly-singlet pseudoscalar [2]. The branching fraction of $J/\psi \rightarrow \gamma A^0$ could be in the range of $10^{-9} - 10^{-7}$ [12], making it accessible at high intensity e^+e^- collider experiments.

The BABAR [13–16], CLEO [17], and CMS [18] experiments have performed searches for A^0 in various decay processes and placed very strong exclusion limits on g_b [10, 15, 16, 18]. The BESIII experiment, on the other hand, is sensitive to g_c . Existing constraints on g_b give $\mathcal{B}(J/\psi \rightarrow A^0) \times \mathcal{B}(A^0 \rightarrow \mu^+ \mu^-) \lesssim 5 \times 10^{-7} \cot^4 \beta$, i.e. $\lesssim 3 \times 10^{-8}$ for $\tan \beta \gtrsim 2$ [11]. The search for the A^0 in J/ψ experiments is particularly important at lower values of $\tan \beta$, typically for $\tan \beta \lesssim 2$.

The BESIII experiment has previously searched for di-muon decays of light pseudoscalars, in the radiative decays of J/ψ using $\psi(2S)$ data, where the pion pair from $\psi(2S) \rightarrow \pi^+ \pi^- J/\psi$ was used to tag the J/ψ events [19]. No candidates were found and exclusion limits on $\mathcal{B}(J/\psi \rightarrow \gamma A^0) \times \mathcal{B}(A^0 \rightarrow \mu^+ \mu^-)$ were set in the range of $(0.4 - 21.0) \times 10^{-6}$ for $0.212 \leq m_{A^0} \leq 3.0 \text{ GeV}/c^2$ [19].

This paper describes the search for a narrow A^0 signal in the fully reconstructed process $J/\psi \rightarrow \gamma A^0$, $A^0 \rightarrow \mu^+ \mu^-$ using $(225.0 \pm 2.8) \times 10^6$ J/ψ events collected by the BESIII experiment in 2009 [20]. The same amount

of generic J/ψ decays, generated by EvtGen [21] where branching fractions of all the known decay processes are taken into account as mentioned in [22], is used for background studies. The A^0 is assumed to be a scalar or pseudo-scalar particle with a very narrow decay width in comparison to the experimental resolution [23].

BESIII is a general purpose spectrometer as described in [24]. It consists of four detector sub-components and has a geometrical acceptance of 93% of the total solid angle. A helium based (40% He, 60% C_3H_8) 43 layer main drift chamber (MDC), operating in a 1.0 T solenoidal magnetic field, is used to measure the momentum of charged particles. Charged particle identification (PID) is based on the time-of-flight (TOF) measured by a scintillation based TOF system, which has one barrel portion and two end-caps, and the energy loss (dE/dx) in the tracking system. Photon and electron energies are measured in a CsI(Tl) electromagnetic calorimeter (EMC), while muons are identified using a muon counter (MUC) system containing nine (eight) layers of resistive plate chamber counters interleaved with steel in the barrel (end-cap) region.

We use simulated signal events with 23 different A^0 mass hypotheses ranging from 0.212 to 3.0 GeV/c^2 to study the detector acceptance and optimize the event selection procedure. The decay of signal events is simulated by the EVTGEN event generator [21], and a phase-space model is used for the $A^0 \rightarrow \mu^+ \mu^-$ decay and a P -Wave model for the decay $J/\psi \rightarrow \gamma A^0$. BABAYAGA 3.5 [25] is used to simulate the radiative Bhabha events, and PHOKHARA 7.0 [26] to simulate initial state radiation (ISR) processes of $e^+e^- \rightarrow \gamma \mu^+ \mu^-$, $e^+e^- \rightarrow \gamma \pi^+ \pi^-$ and $e^+e^- \rightarrow \gamma \pi^+ \pi^- \pi^0$. A Monte Carlo (MC) simulation based on the GEANT4 package [27] is used to determine the detector response and reconstruction efficiencies.

We select events with exactly two oppositely charged tracks and at least one good photon. The minimum energy of this photon is required to be 25 MeV in the barrel region ($|\cos \theta| < 0.8$) and 50 MeV in the end-cap region ($0.86 < |\cos \theta| < 0.92$). The EMC time is also required to be in the range of $[0, 14](\times 50)$ ns to suppress electronic noise and energy deposits unrelated to the signal events. Additional photons are allowed to be in the events. In order to reduce the beam related backgrounds, charged tracks are required to have their points of closest approach to the beam-line within ± 10.0 cm from the interaction point in the beam direction and within 1.0 cm in the plane perpendicular to the beam. In order to have a reliable measurement in the MDC, they must be in the polar angle region $|\cos \theta| < 0.93$. We suppress contamination by electrons by requiring $E_{\text{cal}}^\mu/p < 0.9 c$, where E_{cal}^μ is the energy deposited in the EMC by the showering particles and p is the incident momentum of the charged particles entering the calorimeter. The angle between a photon and the nearest extrapolated track in the EMC is required to be greater than 20 degrees (10 degrees) for $m_{A^0} \leq 0.3 \text{ GeV}/c^2$ ($m_{A^0} > 0.3 \text{ GeV}/c^2$) to remove bremsstrahlung photons.

We assign a muon mass hypothesis to the two charged tracks and require that one of the charged tracks must be identified as a muon using the muon PID system, which is based on the selection criteria: (1) $0.1 < E_{\text{cal}}^{\mu} < 0.3$ GeV, (2) the absolute value of the time difference between TOF and expected muon time (Δt^{TOF}) must be less than 0.26 ns and (3) the penetration depth in MUC must be greater than $(-40.0 + 70 \times p/(\text{GeV}/c))$ cm for $0.5 \leq p \leq 1.1$ GeV/ c and 40 cm for $p > 1.1$ GeV/ c . The two muon candidates are required to meet at a common vertex to form the Higgs candidate. To improve the mass resolution of the A^0 candidates, a four-constraint (4C) kinematic fit is performed with two charged tracks and each of the photons. If there is more than one $\gamma\mu^+\mu^-$ candidate, the one with the minimum 4C χ^2 is selected, and the χ^2 is required to be less than 40 to suppress background contributions from $J/\psi \rightarrow \rho\pi$ and $e^+e^- \rightarrow \gamma\pi^+\pi^-\pi^0$. Fake photons are eliminated by requiring the di-muon invariant mass, obtained from the 4C kinematic fit, to be less than 3.04 GeV/ c^2 . We further require that one of the tracks must have the cosine of the muon helicity angle ($\cos\theta_{\mu}^{\text{hel}}$), defined as the angle between the direction of one of the muons and the direction of J/ψ in the A^0 rest frame, to be less than 0.92 to suppress the backgrounds peaking at $|\cos\theta_{\mu}^{\text{hel}}| \approx 1$.

The above selection criteria select a total of 210,850 events in J/ψ data. Fig. 1 shows the distribution of the reduced di-muon mass, $m_{\text{red}} = \sqrt{m_{\mu^+\mu^-}^2 - 4m_{\mu}^2}$, of data together with the background predictions from various simulated MC samples. m_{red} is equal to twice the muon momentum in the A^0 rest frame, and is easier to model near threshold than the di-muon invariant mass. The background is dominated by the ‘‘non-peaking’’ component of $e^+e^- \rightarrow \gamma\mu^+\mu^-$ and the ‘‘peaking’’ components of $J/\psi \rightarrow \rho\pi$, $\gamma f_2(1270)$, and $\gamma f_0(1710)$.

We perform a series of one dimensional unbinned extended maximum likelihood (ML) fits to the m_{red} distribution to determine the number of signal candidates as a function of m_{A^0} in the interval of $0.212 \leq m_{A^0} \leq 3.0$ GeV/ c^2 . The likelihood function is a combination of signal, continuum background and peaking background contributions from ρ , $f_2(1270)$ and $f_0(1710)$ mesons. To handle the threshold-mass region and peaking backgrounds smoothly, the ML fit is done in intervals $0.002 \leq m_{\text{red}} \leq 0.5$ GeV/ c^2 for $0.212 \leq m_{A^0} \leq 0.4$ GeV/ c^2 , $0.3 \leq m_{\text{red}} \leq 0.65$ GeV/ c^2 for $0.4 < m_{A^0} \leq 0.6$ GeV/ c^2 , $0.4 \leq m_{\text{red}} \leq 1.1$ GeV/ c^2 for $0.6 < m_{A^0} \leq 1.0$ GeV/ c^2 , $0.9 \leq m_{\text{red}} \leq 2.5$ GeV/ c^2 for $1.0 < m_{A^0} \leq 2.4$ GeV/ c^2 and $2.75 \leq m_{\text{red}} \leq 3.032$ GeV/ c^2 for $2.93 < m_{A^0} \leq 3.0$ GeV/ c^2 . We use elsewhere the sliding intervals of $m - 0.2 < m_{\text{red}} < m + 0.1$ GeV/ c^2 , where m is the mean of the m_{red} distribution.

We develop the probability density function (PDF) of signal and backgrounds using the simulated MC events. The signal PDF in the m_{red} distribution is parametrized by the sum of two Crystal Ball (CB) functions [28]. The m_{red} resolution typically varies from 2 to 12 MeV/ c^2

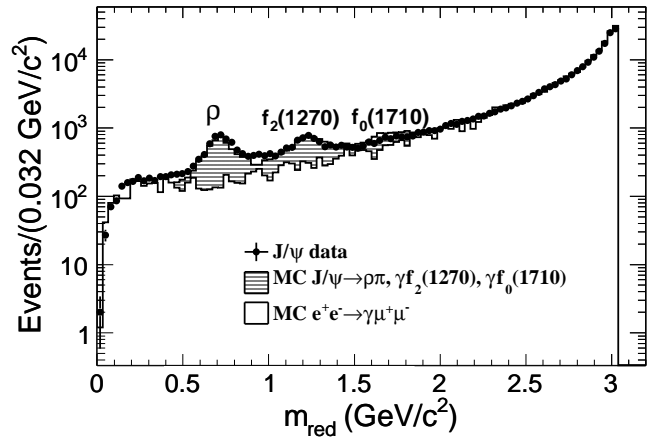


FIG. 1. Distribution of m_{red} for data (black points with error bars), together with the background predictions from the various MC samples, shown by a solid histogram and a histogram with horizontal pattern lines for the non-peaking and peaking backgrounds, respectively. The MC samples are normalized to the data. Three peaking components, corresponding to the ρ , $f_0(1270)$ and $f_0(1710)$ mesons, are observed in the data.

while the signal efficiency varies from 49% to 33% depending upon the momentum values of two muons at different Higgs mass points. The signal efficiency and PDF parameters are interpolated linearly between mass points. We use a polynomial function $\sum_{l=1}^4 p_l m_{\text{red}}^l$ to model the m_{red} distribution of non-peaking background in the threshold mass region of $0.212 \leq m_{A^0} \leq 0.40$ GeV/ c^2 , where p_l are the polynomial coefficients. This higher order polynomial function passes through the origin when $m_{\text{red}} = 0$ and has enough degrees of freedom to provide a threshold like behavior. We use a 2nd (4th and 5th) order Chebyshev polynomial function to describe the m_{red} distribution of non-peaking backgrounds for $0.6 < m_{A^0} \leq 1.0$ GeV/ c^2 and $2.40 < m_{A^0} < 2.75$ GeV/ c^2 ($2.85 \leq m_{A^0} \leq 2.93$ GeV/ c^2 and $2.93 < m_{A^0} \leq 3.0$ GeV/ c^2 , respectively) regions. For the remaining mass regions, we use a 3rd order Chebyshev polynomial function.

The m_{red} distribution of ρ background is described by a ‘Cruiff’ function with a common peak position (μ), independent left and right widths ($\sigma_{L,R}$), and non-Gaussian tails ($\alpha_{L,R}$), whose parameters are determined from the MC $J/\psi \rightarrow \rho\pi$ event sample. The ‘Cruiff’ function is defined as

$$f_{L,R}(m_{\text{red}}) = \exp[-(m_{\text{red}} - \mu)^2 / (2\sigma_{L,R}^2 + \alpha_{L,R}(m_{\text{red}} - \mu)^2)]. \quad (2)$$

The $f_2(1270)$ and $f_0(1710)$ peaking backgrounds are described by the sum of two CB functions using parameters determined from MC samples of $J/\psi \rightarrow \gamma X$, $X \rightarrow \pi^+\pi^-$ decays, where $X = f_2(1270)$ and $f_0(1710)$ mesons.

We search for a narrow resonance in steps of 1.0 MeV/ c^2 in the mass range of $0.22 \leq m_{A^0} \leq$

1.50 GeV/c^2 and 2.0 MeV/c^2 for other mass regions, resulting in a total of 2,035 m_{A^0} points. The shapes of the signal and the peaking background PDFs are fixed while the non-peaking background PDF shape, and the numbers of signal, peaking and non-peaking background events are left free in the fit. The plots of the fit to the m_{red} distribution for selected m_{A^0} points are shown in Fig. 2. Fig. 3 shows signal event (N_{sig}) and the statistical significance, defined as $\mathcal{S} = \text{sign}(N_{\text{sig}}) \sqrt{-2 \ln(\mathcal{L}_0/\mathcal{L}_{\text{max}})}$, as a function of m_{A^0} , where \mathcal{L}_{max} (\mathcal{L}_0) is the maximum likelihood value for a fit with number of signal events being floated (fixed at zero). The distribution of \mathcal{S} is expected to follow the normal distribution under the null hypothesis, consistent with the distribution in Fig. 4. The largest upward local significance is 3.42 σ at $m_{A^0} = 2.918 \text{ GeV}/c^2$.

We repeat the search using a polynomial function $\sum_{l=1}^5 p_l m_{\text{red}}^l$ for $m_{A^0} \leq 0.4 \text{ GeV}/c^2$ and an alternative higher order Chebyshev polynomial function for other mass regions to model the non-peaking background. The difference between the absolute values of two N_{sig} is considered as an additive systematic uncertainty at each mass point. An additive uncertainty reduces the significance of any observed signal and does not scale with the number of reconstructed signal events.

We study a large ensemble of pseudo-experiments, based on the aforementioned PDFs, to validate the fit procedure and compute the bias of the ML fit. The bias arises due to the imperfections in modeling the signal PDFs and the low statistics of the ML estimate. The value of the fit bias is found to be 0.21 events and considered to be an additive systematic uncertainty. We further use the pseudo-experiments to estimate the probability of observing a fluctuation of $\mathcal{S} \geq 3.42\sigma$, which is found to be 26.0%. The corresponding global significance of such an excess anywhere in the full m_{A^0} range is 0.64 σ ; we therefore conclude that no evidence of A^0 production is found at any mass points.

The uncertainty due to fixed signal and tail PDF parameters used for the ρ , $f_2(1270)$ and $f_0(1710)$ peaking backgrounds in data, is observed to be (0.0 – 1.64) events after varying each parameter within its statistical uncertainties while taking correlations between the parameters into account. The mean and sigma values of the peaking backgrounds are corrected using a high statistics control sample of the same decay process in which all the selection criteria, developed in this work, are applied except that of the penetration depth in MUC. We assign 50% of the relative difference in resolution values of peaking backgrounds between data and MC as a systematic uncertainty, which is considered as a source of multiplicative systematic uncertainty. Multiplicative uncertainties scale with the number of reconstructed signal events and do not reduce the significance of any observed signal, but degrade the upper limit values. They arise due to the reconstruction efficiency, the uncertainty in the number of J/ψ mesons (1.3%), muon tracking efficiency (1.0% per track) and resolution of peaking backgrounds (1.2% for

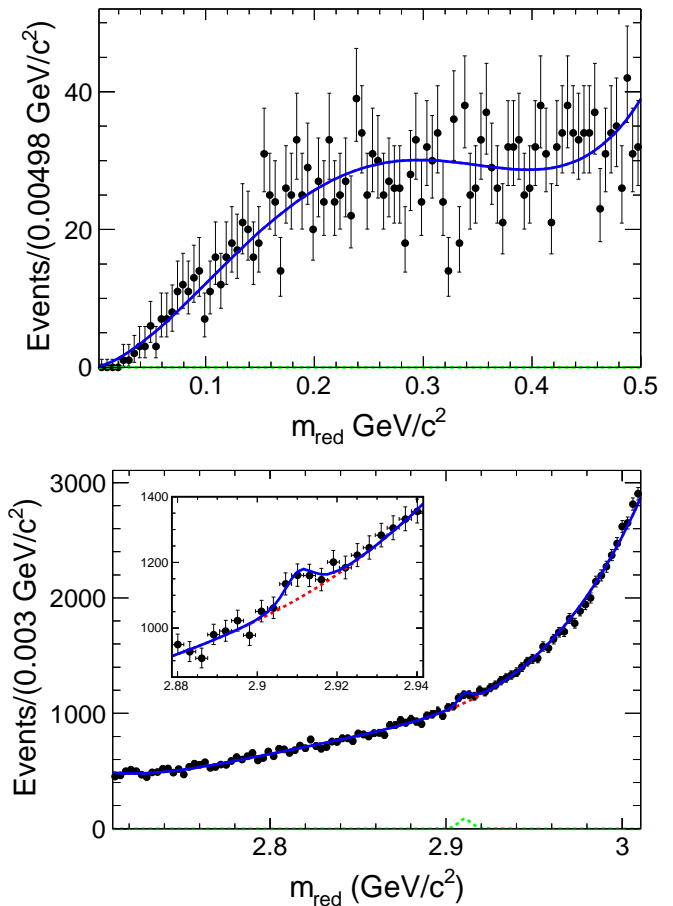


FIG. 2. (color online) Plot of the fit to the m_{red} distribution for (top) $m_{A^0} = 0.212 \text{ GeV}/c^2$ and (bottom) $m_{A^0} = 2.918 \text{ GeV}/c^2$. The contribution of non-peaking background is shown by a red dashed line, the signal PDF by a green dotted line (seen only in the bottom figure) and total PDF by a blue solid line. Due to limited statistics in the low-mass region as shown in the top figure, we allow the signal events to be floated for positive N_{sig} only during the fit. The inlay in the upper left of Fig. (bottom) displays an enlargement of the m_{red} region between 2.88 and 2.94 GeV/c^2 . The largest upward local significance is observed to be 3.42 σ at $m_{A^0} = 2.918 \text{ GeV}/c^2$ point.

the ρ resonance and 6.52% for $f_2(1270)$ and $f_0(1710)$ resonances).

We measure the photon reconstruction systematic uncertainty to be better than 1.0% using a $e^+e^- \rightarrow \gamma\mu^+\mu^-$ sample in which the ISR photon momentum is estimated using the four-momenta of two charged tracks [29]. We use a $J/\psi \rightarrow \mu^+\mu^-(\gamma)$ control sample, where one track is tagged with tight muon PID and photons are produced via final state radiation, to study the systematic uncertainty associated with the muon PID ((4.0–5.73)%, χ_{4C}^2 (1.56%) and the $\cos\theta_{\mu}^{\text{hel}}$ (0.34%) requirements. The final muon PID uncertainty also takes into account the fraction of events with one track or two tracks identified as

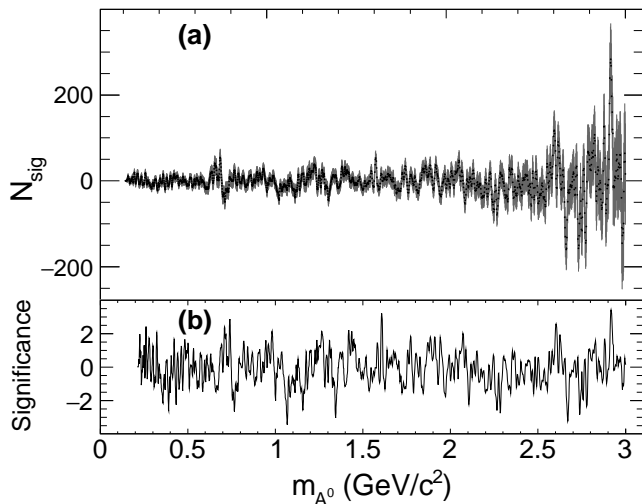


FIG. 3. (a) Number of signal events (N_{sig}) and (b) signal significance (S) obtained from the fit as a function of m_{A^0} .

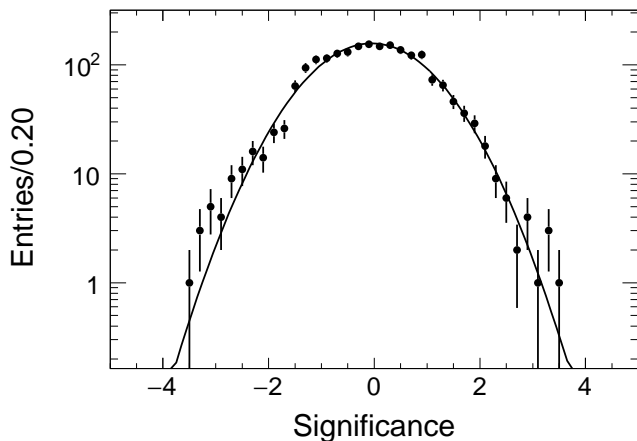


FIG. 4. Histogram of the statistical significance S obtained from the fit at $2,035 m_{A^0}$ points, together with the expected S distribution in the absence of signal, which is shown by the solid curve.

muons, which is obtained from the signal MC. The total multiplicative systematic uncertainty varies in the range of $(5.03 - 9.20)\%$ depending on m_{A^0} .

We compute the 90% confidence-level (C.L.) upper limits on the product branching fractions of $\mathcal{B}(J/\psi \rightarrow \gamma A^0) \times \mathcal{B}(A^0 \rightarrow \mu^+ \mu^-)$ as a function of m_{A^0} using a Bayesian method [22]. The systematic uncertainty is incorporated by convolving the negative log likelihood (NLL) versus branching fraction curve with a Gaussian distribution having a width equal to the systematic uncertainty. The limits range between $(2.8 - 495.3) \times 10^{-8}$ for the Higgs mass region of $0.212 \leq m_{A^0} \leq 3.0 \text{ GeV}/c^2$ depending on the A^0 mass points, as shown in Fig. 5.

We also compute $g_b (= g_c \tan^2 \beta) \times$

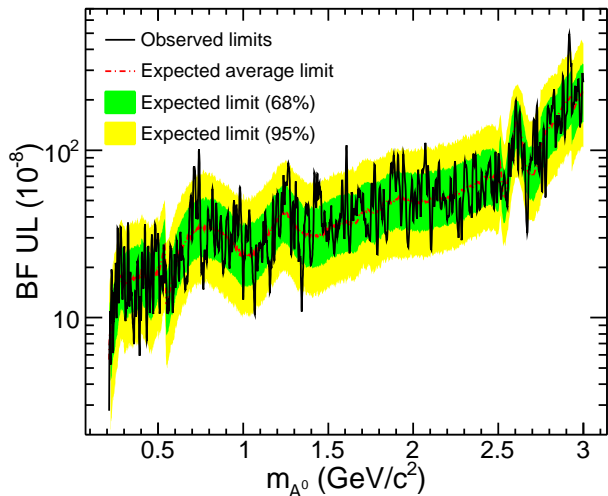


FIG. 5. (color online) The 90% C.L. upper limits (UL) on the product branching fractions $\mathcal{B}(J/\psi \rightarrow \gamma A^0) \times \mathcal{B}(A^0 \rightarrow \mu^+ \mu^-)$ as a function of m_{A^0} including all the uncertainties (solid line), together with expected limits computed using a large number of pseudo-experiments. The inner and outer bands include statistical uncertainties only and contain 68% and 95% of the expected limit values. The average dashed line in the center of the inner band is the expected average upper limit of 1600 pseudo-experiments. A better sensitivity in the mass region of $0.212 \leq m_{A^0} \leq 0.22 \text{ GeV}/c^2$ is achieved due to almost negligible backgrounds as seen in Fig. 2 (top).

$\sqrt{\mathcal{B}(A^0 \rightarrow \mu^+ \mu^-)}$ [11] for different values of $\tan \beta$ using Equation 1 to compare our results with the BABAR measurement [16]. This new result seems to be better than the BABAR measurement [16] in the low-mass region for $\tan \beta \leq 0.6$ (Fig. 6 (a)). Our results are thus complementary to those obtained by considering the b -quark [10, 16]. Both types of constraints may then be combined so as to provide, *independently of $\tan \beta$* , an upper limit on $\cos \theta_A (= |\sqrt{g_b g_c}|) \times \sqrt{\mathcal{B}(A^0 \rightarrow \mu^+ \mu^-)}$ computed using the method of Ref. [11], as a function of m_{A^0} , as shown in Fig. 6 (b). This combined limit varies in the range of $0.034 - 0.249$ for $0.212 \leq m_{A^0} \leq 3.0 \text{ GeV}/c^2$.

In summary, we find no significant signal for a light Higgs boson in the radiative decays of J/ψ and set 90% C.L. upper limits on the product branching fraction of $\mathcal{B}(J/\psi \rightarrow \gamma A^0) \times \mathcal{B}(A^0 \rightarrow \mu^+ \mu^-)$ in the range of $(2.8 - 495.3) \times 10^{-8}$ for $0.212 \leq m_{A^0} \leq 3.0 \text{ GeV}/c^2$. This result, a factor of 5 times improvement over the previous BESIII measurement [19], is in agreement with the theoretical expectation $\lesssim 5 \times 10^{-7} \cot^4 \beta$ from [11], but better than the BABAR measurement [16] in the low-mass region for the $\tan \beta \leq 0.6$. The combined limits on $\cos \theta_A \times \sqrt{\mathcal{B}(A^0 \rightarrow \mu^+ \mu^-)}$ for the BABAR [16] and BESIII measurements reveal that the A^0 is constrained to be mostly singlet.

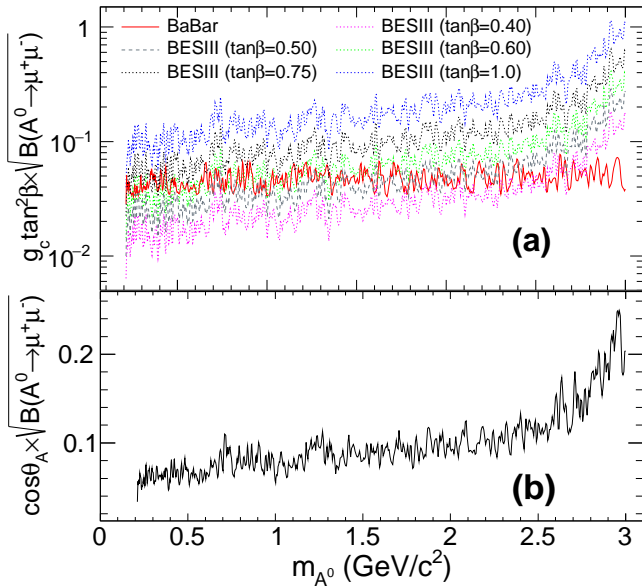


FIG. 6. (color online) (a) The 90% C.L. upper limits on $g_b(= g_c \tan^2 \beta) \times \sqrt{\mathcal{B}(A^0 \rightarrow \mu^+ \mu^-)}$ for the BABAR [16] and BESIII measurements and (b) $\cos \theta_A(= |\sqrt{g_b g_c}|) \times \sqrt{\mathcal{B}(A^0 \rightarrow \mu^+ \mu^-)}$ as a function of m_{A^0} . We compute $g_c \tan^2 \beta \times \sqrt{\mathcal{B}(A^0 \rightarrow \mu^+ \mu^-)}$ for different values of $\tan \beta$ to compare our results with the BABAR measurement [16].

I. ACKNOWLEDGEMENT

The authors wish to thank Pierre Fayet for helpful discussions of new physics models. The BESIII collaboration thanks the staff of BEPCII and the IHEP computing center for their strong support. This work is supported in part by National Key Basic Research Program of China under Contract No. 2015CB856700; National Natural Science Foundation of China (NSFC) under Contracts Nos. 11125525, 11235011, 11322544, 11335008, 11425524; the Chinese Academy of Sciences (CAS) Large-Scale Scientific Facility Program; the CAS Center for Excellence in Particle Physics (CCEPP); the Collaborative Innovation Center for Particles and Interactions (CICPI); Joint Large-Scale Scientific Facility Funds of the NSFC and CAS under Contracts Nos. 11179007, U1232201, U1332201; CAS under Contracts Nos. KJCX2-YW-N29, KJCX2-YW-N45; 100 Talents Program of CAS; National 1000 Talents Program of China; INPAC and Shanghai Key Laboratory for Particle Physics and Cosmology; German Research Foundation DFG under Contract No. Collaborative Research Center CRC-1044; Istituto Nazionale di Fisica Nucleare, Italy; Joint Funds of the National Science Foundation of China under Contract No. U1232107; Ministry of Development of Turkey under Contract No. DPT2006K-120470; Russian Foundation for Basic Research under Contract No. 14-07-91152; The Swedish Research Council; U. S. Department of Energy under Contracts Nos. DE-FG02-04ER41291, DE-FG02-05ER41374, DE-SC0012069, DESC0010118; U.S. National Science Foundation; University of Groningen (RuG) and the Helmholtzzentrum fuer Schwerionenforschung GmbH (GSI), Darmstadt; WCU Program of National Research Foundation of Korea under Contract No. R32-2008-000-10155-0.

-
- [1] F. Wilczek, Phys. Rev. Lett. **39**, 1304 (1977); Phys. Rev. Lett. **40**, 279 (1978).
 [2] P. Fayet, Nucl. Phys. B **187**, 184 (1981); H. B. Li and T. Luo, Phys. Lett. B **686**, 249 (2010).
 [3] P. Fayet, Nucl. Phys. B **90**, 104 (1975); M. Maniatis, Int. J. Mod. Phys. A **25**, 3505–3602 (2010); U. Ellwanger, C. Hugonie and A.M. Teixeira, Phys. Reports **496**, 1–77 (2010).
 [4] H. E. Haber and G. L. Kane, Phys. Rep. **117**, 75 (1985).
 [5] A. Delgado, C. Kolda, A. D. Puente, Phys. Lett. B **710**, 460 (2012).
 [6] M. L. Mangano and P. Nason, Mod. Phys. Lett. **A 22**, 1373 (2007).
 [7] P. Nason, Phys. Lett. B **175**, 223 (1986).
 [8] R. Barbieri, R. Gatto, R. Kogerler, and Z. Kunszt, Phys. Lett. B **57**, 455 (1975).
 [9] M. Beneke, A. Signer and V. A. Smirnov, Phys. Rev. Lett. **80**, 2535 (2009).
 [10] R. Dermisek and J. F. Gunion, Phys. Rev. D **81**, 075003 (2010); F. Domingo, JHEP **1104**, 016 (2011).
 [11] P. Fayet, Phys. Rev. D **75**, 115017 (2007); Phys. Lett. B **675**, 267 (2009).
 [12] R. Dermisek, J. F. Gunion and B. McElrath, Phys. Rev. D **76**, 051105 (2007).
 [13] B. Aubert *et al.* [BABAR Collaboration], Phys. Rev. Lett. **103**, 081803 (2009); Phys. Rev. Lett. **103**, 181801 (2009).
 [14] P. del Amo Sanchez *et al.* [BABAR Collaboration], Phys. Rev. Lett. **107**, 021804 (2011).
 [15] J. P. Lees *et al.* [BABAR Collaboration], Phys. Rev. Lett. **107**, 221803 (2011); Phys. Rev. D **88**, 071102(R) (2013); Phys. Rev. D **88**, 031701(R) (2013); Phys. Rev. D **91**, 071102(R) (2015).
 [16] J. P. Lees *et al.* [BABAR Collaboration], Phys. Rev. D **87**, 031102(R) (2013).
 [17] W. Love *et al.* [CLEO Collaboration], Phys. Rev. Lett. **101**, 151802 (2008).
 [18] S. Chatrchyan *et al.* [CMS collaboration], Phys. Rev. Lett. **109**, 121801 (2012).

- [19] M. Ablikim *et al.* [BESIII collaboration], Phys. Rev. D **85**, 092012 (2012).
- [20] M. Ablikim *et al.* (BESIII Collaboration), Chinese Phys. C (HEP & NP) **36**(10), 915 (2012).
- [21] D. J. Lange, Nucl. Instrum. Meth. A **462**, 152 (2001).
- [22] K.A. Olive *et al.* (Particle Data Group), Chinese Phys. C **38**, 090001 (2014).
- [23] E. Fullana and M.A. Sanchis-Lozano, Phys. Lett. B **653**, 67 (2007).
- [24] M. Ablikim *et al.* (BESIII Collaboration), Nucl. Instr. and Methods A **614**, 345 (2010).
- [25] G. Balossini, C. M. Carloni calame, G. Montagna, O. Nicosini and F. Piccinini, Nucl. Phys. B **758**, 227 (2006).
- [26] H. Czyz, A. Grzelinska, A. Wapienik, Acta Phys. Polon B **34**, 5219 (2003).
- [27] S. Agostinelli *et al.* [GEANT4 Collaboration], Nucl. Instrum. Methods Phys. Res., Sect. A **506**, 250 (2003).
- [28] M. J. Oreglia, Ph.D Thesis, report SLAC-236 (1980); J.E. Gaiser, Ph.D Thesis, report SLAC-255 (1982); T. Skwarnicki, Ph.D Thesis, report DESY F31-86-02 (1986).
- [29] V. Prasad, C. X. Liu, X. B. Ji, W. D. Li, H. M. Liu and X. C. Lou, Springer Proceed. in Phys. **174**, 577 (2016).